nature geoscience

LETTERS

PUBLISHED ONLINE: 11 MARCH 2012 | DOI: 10.1038/NGEO1414

Shallow axial magma chamber at the slow-spreading Erta Ale Ridge

Carolina Pagli[1]*, Tim J. Wright[1], Cynthia J. Ebinger[2], Sang-Ho Yun[3], Johnson R. Cann[1], Talfan Barnie[4] and Atalay Ayele[5]

The existence of elongated, shallow magma chambers beneath the axes of fast-spreading mid-ocean ridges is well established[1–8]. Yet, at slow-spreading ridges such shallow and elongated magma chambers are much less evident[9,10]. Simple thermal models[8] therefore predict that spreading velocity and magma supply may provide the main controls on magma-chamber depth and morphology. Here we use interferometric synthetic aperture radar data to investigate the dynamics of the magma chamber beneath the slow-spreading Erta Ale segment of the Ethiopian Rift. We show that an eruption from Alu–Dalafilla in November 2008 was sourced from a shallow, 1 km deep, elongated magma chamber that is divided into two segments. The eruption was probably triggered by a small influx of magma into the northern segment. Both segments of the magma chamber fed the main eruption through a connecting dyke and both segments have been refilling rapidly since the eruption ended. Our results support the presence of independent sources of magma supply to segmented chambers located along the axes of spreading centres[11]. However, the existence of a shallow, elongated axial chamber at Erta Ale indicates that spreading rate and magma supply may not be the only controls on magma-chamber characteristics.

Shallow (<2 km depth) elongated axial magma chambers have been detected at many places on fast-spreading ridges[1–7], but magma chambers have been found at only a few slow-spreading ridges as deeper isolated magma pockets[9,10]. The depth and continuity of these chambers is thought to depend on spreading rate and magma supply[8].

Typically, an axial high and continuous shallow magma chamber (at ~1–2 km depth) characterizes ridges spreading faster than ~40 mm yr^{-1} (refs 1,2,8), whereas a median valley and isolated deeper chambers (≥3 km deep) are found at slower-spreading ridges[5,9,10]. Elongated axial magma chambers are typically 250–4,000 m wide[1,3,4] and tens of kilometres long. In contrast, the magma chambers at slow-spreading ridges are isolated, near-spherical bodies. Magma chambers at ~3 km depth have been inferred both in Krafla[12] and Askja[13], Iceland. At the Dabbahu segment in Afar, both the Gabho and Dabbahu volcanoes are also associated with axisymmetric chambers between 3 and 5 km depth[14]. The ~120-km-long Erta Ale spreading segment separates the Nubian plate from the Danakil microplate in the Afar region of Ethiopia. It forms a continuous ridge made up of distinct volcanic centres[15] (Fig. 1a,b), including the Erta Ale volcano, which hosts an active lava lake[15,16]. The spreading rate at this latitude is estimated at ~12 mm yr^{-1} (ref. 17). In November 2008, an eruption occurred in the Alu–Dalafilla volcanic centre that lies 30 km north of the

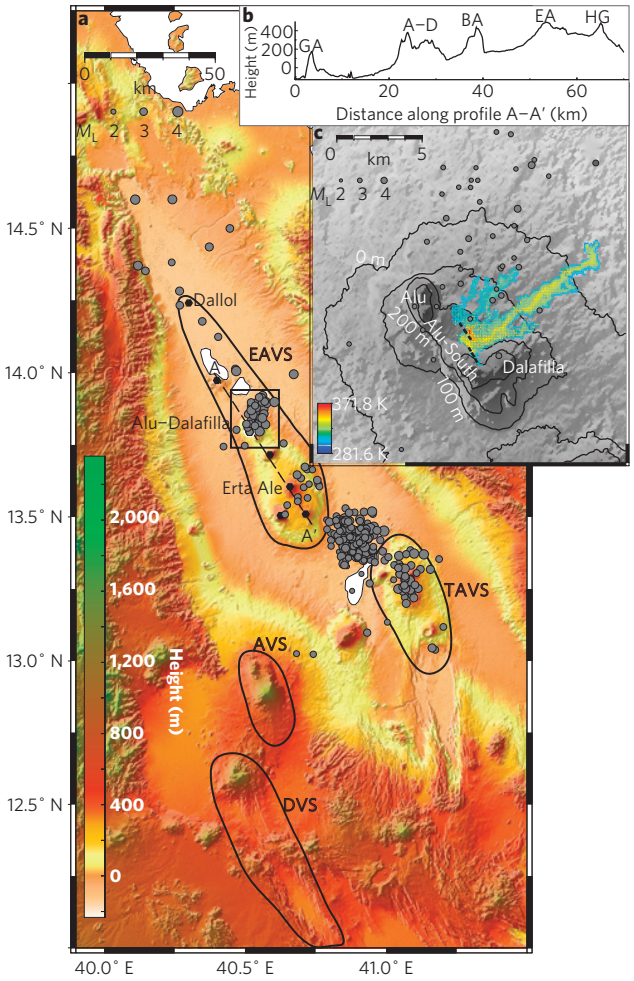

Figure 1 | Location of the Erta Ale volcanic segment. a, Afar depression (Ethiopia). EAVS, Erta Ale volcanic segment; TAVS, Tat Ale volcanic segment; AVS, Alayta volcanic segment; DVS, Dabbahu volcanic segment. Circles represent earthquakes 2007–2009 in EAVS and TAVS. Hexagons mark volcanic centres of EAVS and the box marks the study area in **c**. **b**, Topography cross-section along A–A′, as marked in **a**. Volcanic centres: GA, Gada Ale; A–D Alu–Dalafilla; BA, Bora Ale; EA, Erta Ale; HG, Haily Gubbi. **c**, Alu–Dalafilla, the coloured area is the surface temperature of the lava flow erupted in 2008. The circles represent earthquakes from 2–3 November 2008.

[1]School of Earth and Environment, University of Leeds, Leeds LS2 9JT, UK, [2]Department of Earth & Environmental Sciences, University of Rochester, Rochester, New York 14627, USA, [3]Jet Propulsion Laboratory, California Institute of Technology, Pasadena, California 91109, USA, [4]Department of Geography, University of Cambridge, Cambridge CB2 3EN, UK, [5]Institute of Geophysics, Space Science and Astronomy, Addis Ababa University, Addis Ababa, Ethiopia. *e-mail: C.Pagli@leeds.ac.uk.

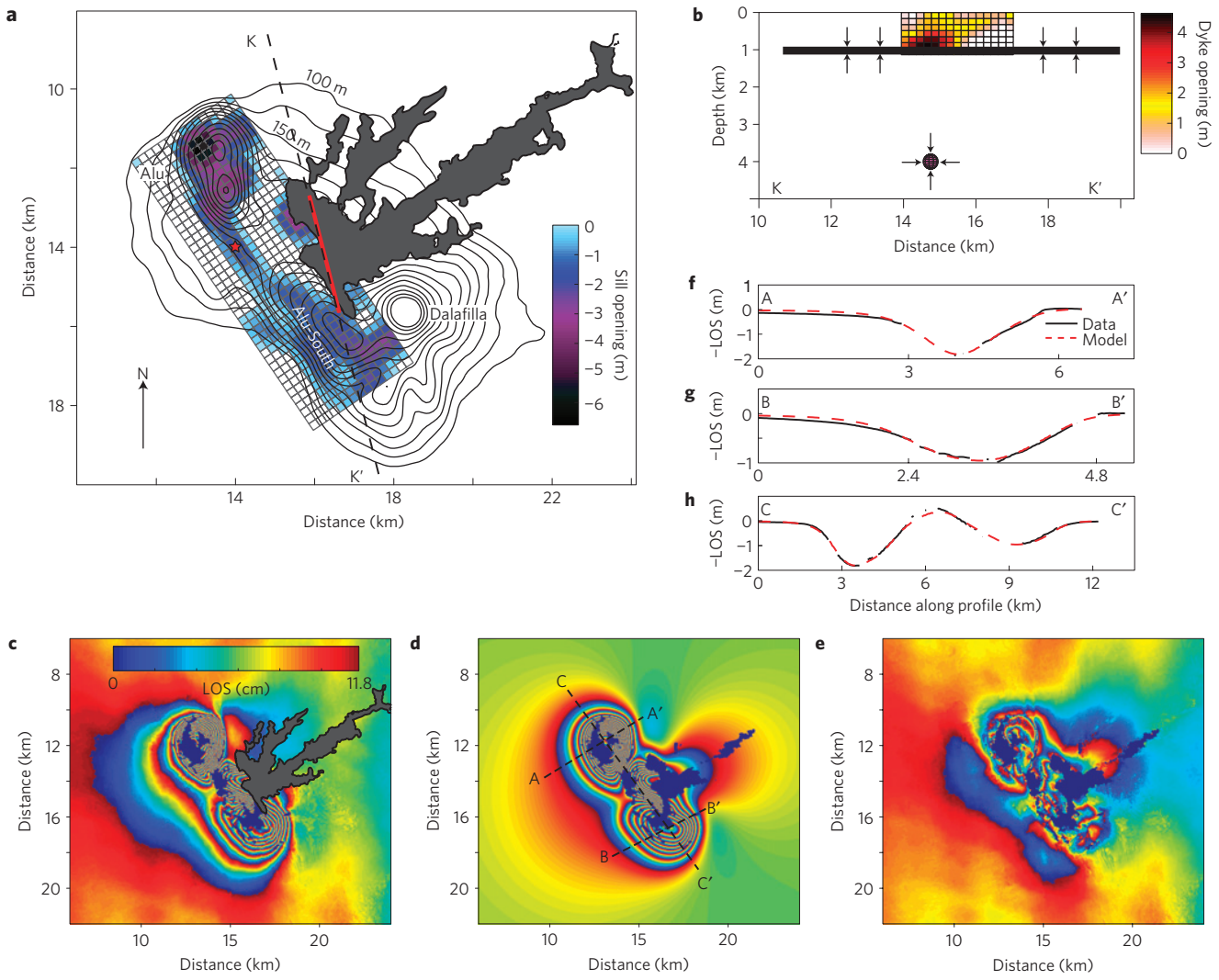

Figure 2 | Co-eruptive InSAR data and models. a, Plan view of the co-eruptive distributed sill contraction, overlaid by topographic contours and the lava flow. The red line represents the dyke and the red star the Mogi. **b** Cross-section of the distributed dyke opening, the location of which is shown by the dashed line K–K′ in **a**. The black line represents the projection of the sill and the sphere is the Mogi. **c**, ALOS ascending co-eruptive interferogram, **d**, model interferogram and **e**, residual. One colour cycle represents 11.8 cm of displacement in the satellite line of sight (LOS). **f**–**h**, Observed and modelled displacements along cross-sections shown in **d**.

lava lake. Alu–Dalafilla includes the basaltic volcanic cone, Alu, a 3-km-long basaltic volcanic range, here named Alu-South, and a silicic stratovolcano, Dalafilla (Fig. 1c). Fumarolic activity was observed at some of these faults in Alu and in the Dalafilla crater in 1968 (ref. 15) but there has been no report of any volcanic eruption in the Erta Ale segment since the first observations in 1907, except for overflow events from the Erta Ale lava lake[18,19].

Detectable but infrequent earthquakes occurred on 30 October and recommenced at 11:10 UTC on 3 November 2008. By 12:22 UTC, their frequency and magnitude increased (Supplementary Figs S1 and S2)[20]. Nearly continuous swarms of local magnitude (M_L) < 4 earthquakes between 12:22 and 12:55 UTC are interpreted as surface faulting above a propagating dyke (Supplementary Fig. S2) that led to the eruption. This is in agreement with the appearance of thermal anomalies in Meteosat SEVIRI images between 12:57 and 13:12 UTC on 3 November 2008. ASTER thermal infrared images from NASA's Terra satellite show that two en-echelon eruptive fissures opened southeast of Alu and lava flowed towards the east and north of Dalafilla (Fig. 1c). OMI sulphur dioxide[21] and MODIS thermal[22] images show that a volcanic plume originated from the eruptive fissures on 3 November and drifted northeastwards. We lack direct observations of the eruption but based on a combined analysis of satellite images and seismicity we deduce that the eruption started on 3 November and eruptive activity peaked over a few hours and then waned exponentially until stopping on the night of 6 November 2008. Here, we study the surface deformation before, during and after the Alu–Dalafilla eruption using an extensive interferometric synthetic aperture radar (InSAR) data set. From this information we are able to provide the first evidence for a shallow (<2 km deep) elongated axial magma chamber at a subaerial slow-spreading segment and to determine its shallow crustal magmatic plumbing system. Furthermore, we are able to observe the dynamic behaviour of an elongated axial magma chamber for the first time.

We formed a time series of interferograms using radar images acquired by the ENVISAT satellite, from five different tracks both in descending and ascending orbits. We also used data acquired by the ALOS satellite covering the co-eruptive period (Fig. 2). In particular, acquisitions made on 3 November and 5 November 2008 are used to detect changes in the style of crustal deformation during the eruption.

Pre-eruptive interferograms show that a 3-km-diameter area centred over the Alu volcano uplifted at a rate of ~3 cm per month

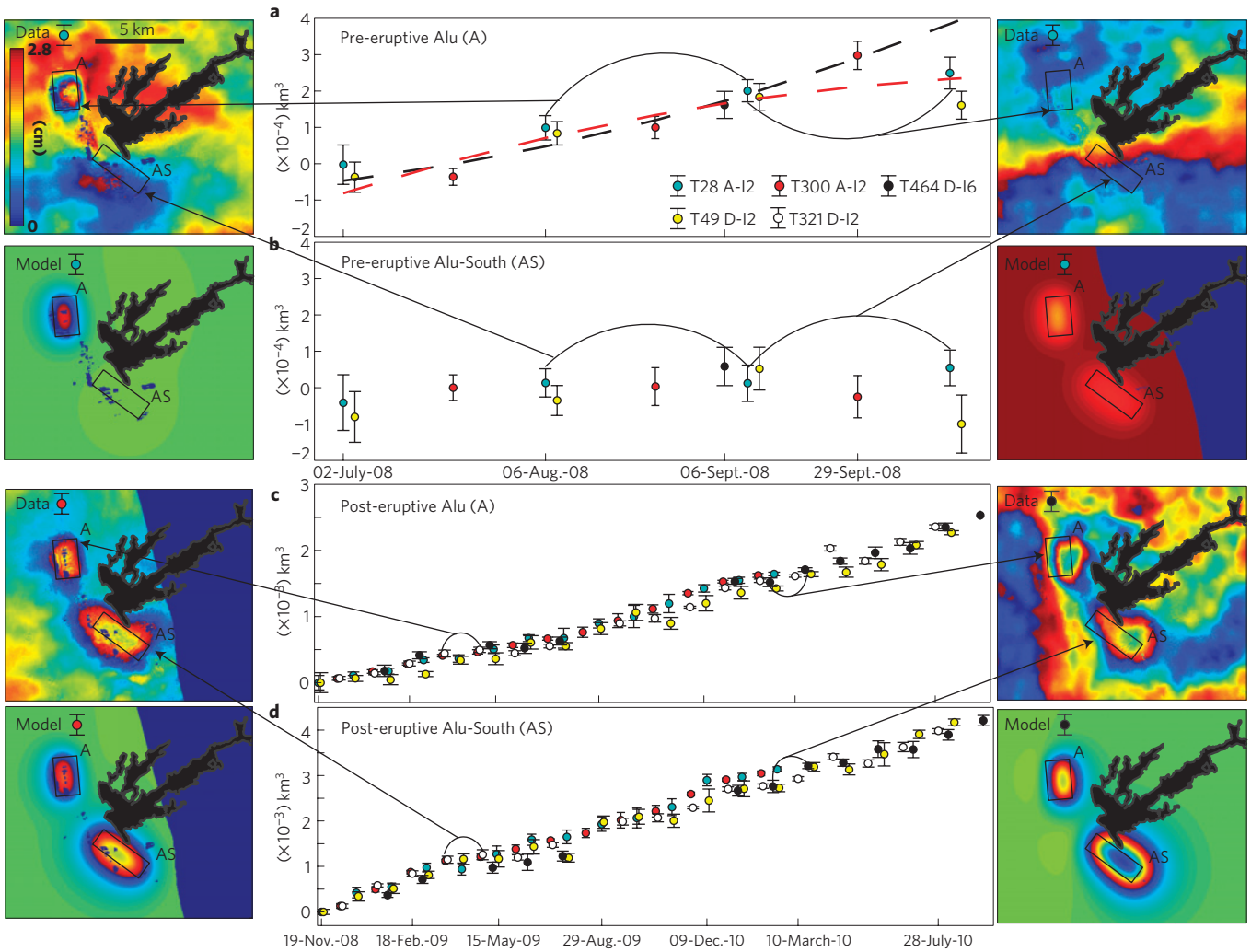

Figure 3 | Time-evolving cumulative volume changes. a,**b**, Pre-eruptive and **c**,**d**, post-eruptive periods. Circles represent acquisitions colour-coded to satellite track number, orbit and mode (for example A-I2, ascending orbit in mode 2). The red dashed line in **a** represents the best-fit curve using all the data, whereas the black dashed line is the best-fit curve excluding the last two circles. The lines highlight the different deformation patterns, uplift July–September 2008 but quiescence a month before the eruption. Selected interferograms and their models are shown for given time intervals on the sides. The colour bar shown in the upper left corner applies to all interferograms.

from July to September 2008 (Fig. 3a). The inflation ceased by 29 September and no significant deformation was observed in Alu until 17 October 2008. No deformation was detected at Alu-South (Fig. 3b) or Dalafilla before the eruption.

Co-eruptive interferograms show an elongated, ~10-km-long, subsidence signal with two closely spaced maxima centred at the Alu volcano, with maximum subsidence of 1.9 m, and at Alu-South, maximum subsidence of 1 m (Fig. 2). The largest subsidence occurred at both volcanoes during the first day of eruption but significant subsidence, up to ~0.5 m, followed from 3 November to 5 November. From 5 November the deformation pattern at Alu-South reversed and uplift started, whereas at Alu minor subsidence continued between 5 November and 19 November but subsequently reversed to uplift. Since then, uplift occurred both at Alu and Alu-South. We initially analysed the co-eruptive deformation to determine how many and what type of magmatic sources played a role during the eruption. To match the observed deformation, we required three distinct sources: a shallow sill at ~1 km depth extending from Alu to Alu-South; a dyke at the location of the eruptive fissure; and a deflating magma chamber (Mogi source) at 4 km depth between Alu and Alu-South (Fig. 2, Supplementary Fig. S4 and Supplementary Information)[23]. The model explains 98% of the data variance. The maximum dyke opening was 4.6 m and the total dyke volume was 5.1×10^6 m^3, whereas the maximum sill contraction was 6.7 m. The maximum dyke opening occurred at the northern end, close to Alu, where the largest deflation is also observed. The total deflating volumes of the sill and the magma chamber were 23.2×10^6 m^3 and 7.3×10^6 m^3, respectively. The lava flow covers an area of $\sim 16 \times 10^6$ m^2 but we lack measurements of its thickness to derive the exact eruptive volume. However, an average thickness of ~1.6 m is required to match the sum of the deflating and the intruded volumes, of 25.4×10^6 m^3.

As the pre-eruptive inflation volume was only 0.4×10^6 m^3, this implies that most of the erupted magma must have been already present at shallow levels, in the uppermost 4 km, before the eruption, unless magma moved rapidly from a deep source (>10 km) to the shallow chamber between 18 October and 2 November. We consider the second hypothesis unlikely, as Alu–Dalafilla was seismically quiet in this period and two $M_L \sim 3$ earthquakes on 30 October are the only significant precursory signals. We do not see any clear signal from the 4-km-deep reservoir or any deeper source in the pre- and post-eruptive periods and it seems that the two shallow sills were the only sources of

deformation. These periods were analysed with a time-evolving least squares inversion approach[24]. We fixed the geometries of magmatic bodies derived from the nonlinear inversion of the co-eruptive deformation (Supplementary Information) and inverted a series of 90 interferograms for the time-dependent opening/contraction of the sills (Fig. 3). A time period of more than two years, from June 2008 to September 2010, was analysed. Uncertainties on the model parameters were estimated using a Monte Carlo simulation of correlated noise[25].

Our modelling results show that only the part of the sill below Alu inflated before the eruption (Fig. 3a,b). In contrast, the whole sill under Alu and Alu-South deflated during the eruption when magma moved out. This indicates that the sill was always present in the area but had become divided into two parts. Before the eruption, only Alu was linked to a deep reservoir and the renewed magma influx there triggered the dyke intrusion, which established a connection between the two previously disconnected chambers. The replenishment phase started in Alu-South from 5 November 2008, but from 19 November 2008 in Alu, indicating that independent links between a deep reservoir and the two portions of the chamber were established during that period. However, from 19 November 2008 (Fig. 3c,d) both Alu and Alu-South have followed a similar replenishment pattern, suggesting that the magma chambers are behaving as a connected body at present. The magma inflow in Alu reached $\sim 2.5 \times 10^6$ m^3 and at Alu-South $\sim 4.5 \times 10^6$ m^3 ($\sim$30% of the co-eruptive volume) by September 2010. The replenishment pattern in Fig. 3c,d could be divided into three phases lasting two to four months, indicating that magma may have flown in pulses rather than continuously. However, these fluctuations are small compared with the error bars and future studies are needed to confirm this hypothesis. No significant deformation signals or seismic activity were observed at the Erta Ale volcano before, during, or after the Alu–Dalafilla eruption, indicating that the shallow magmatic systems at Alu–Dalafilla and at Erta Ale are not linked at present.

We note that if, before the eruption, the Alu–Dalafilla chamber was only $\sim$4 m thick (the average co-eruptive deflation) it would have completely solidified in about 20 days (Supplementary Information)[26]. Given that the chamber's pre-eruptive inflation volume was less than 2% of the co-eruptive deflation, it must have remained molten at least since the last recharge event. This implies a much thicker sill (for example a 160 m sill cools in 100 years) and/or that the magma chamber is regularly replenished by new melt.

The active volcanic segments of Afar show different styles of magmatism[27], as also observed at some submerged ridges[28]. Erta Ale is dominated by magmatic construction and the rift axis is a topographic high, whereas at the Dabbahu segment (Fig. 1) dykes and faulting have induced subsidence, leading to the formation of an axial graben. Furthermore, at Dabbahu, magma seems to be located in isolated chambers at depths $\sim$3 km beneath distinct volcanic centres[2,14], rather than in a shallow elongated axial system as found at Alu–Dalafilla.

The main control on axial morphology and depth of axial magma chambers at mid-ocean ridges has commonly been attributed to spreading velocity and variable magma supply[2,5,8,28]. Phipps Morgan and Chen[8] modelled the thermal structures of mid-ocean ridges as a balance between heat addition by magma intrusion and heat removal by hydrothermal circulation. On the basis of this modelling, a 1-km-deep elongated axial magma chamber at the Erta Ale segment should not exist—a chamber of >4 km depth would be expected, given the spreading rate of 12 mm yr^{-1} (ref. 17) and crustal thickness of 15 km (ref. 29). However, a key feature of this model[8] is the intense hydrothermal circulation, which provides an efficient way of cooling the magma chamber. The relative lack of water and/or a vigorous hydrothermal circulation in desert environments such as Erta Ale may be responsible for the presence of magma chambers at this unexpectedly shallow depth. Other reasons that could explain the persistence of a magma chamber at 1 km depth in Alu–Dalafilla include excessive magma production in the region, high frequency of magma-chamber replenishment, and/or the proximity to the Afar plume[30].

Received 2 November 2011; accepted 3 February 2012; published online 11 March 2012

References

1. Carbotte, S. M., Mutter, C., Mutter, J. & Ponce-Correa, G. Influence of magma supply and spreading rate on crustal magma bodies and emplacement of the extrusive layer: Insights from the East Pacific Rise at lat 16N. *Geology* **26,** 455–458 (1998).
2. Macdonald, K. C., Sempere, J-C. & Fox, P. J. East Pacific Rise from Siqueiros to Orozco Fracture Zone: Along-strike continuity of axial neo-volcanic zone and structure and evolution of overlapping spreading centres. *J. Geophys. Res.* **89,** 6049–6069 (1984).
3. Detrick, R. S. *et al.* Multi-channel seismic imaging of a crustal magma chamber along the East Pacific Rise. *Nature* **326,** 35–41 (1987).
4. Singh, S. C. *et al.* Seismic reflection images of the Moho underlying melt sills at the East Pacific Rise. *Nature* **442,** 287–290 (2006).
5. Purdy, G. M., Kong, L. S. L., Christeson, G. L. & Solomon, S. C. Relationship between spreading rate and the seismic structure of mid-ocean ridges. *Nature* **355,** 815–817 (1992).
6. Dunn, R. A. & Toomey, D. R. Seismological evidence for three-dimensional melt migration beneath the East Pacific Rise. *Nature* **388,** 259–262 (1997).
7. Detrick, R. S. *et al.* Seismic structure of the southern East Pacific Rise. *Science* **259,** 499–503 (1993).
8. Phipps Morgan, J. & Chen, Y. J. Dependence of ridge-axis morphology on magma supply and spreading rate. *Nature* **364,** 706–708 (1993).
9. Sinha, M. C. *et al.* Evidence for accumulated melt beneath the slow spreading Mid-Atlantic Ridge. *Phil. Trans. R. Soc. Lond. A* **355,** 233–253 (1997).
10. Singh, C. S. Discovery of a magma chamber and faults beneath a Mid-Atlantic Ridge hydrothermal field. *Nature* **442,** 1029–1032 (2006).
11. Castillo, P. *et al.* Petrology and Sr, Nd, and Pb isotope geochemistry of mid-ocean ridge basalt glasses from the 11° 45′N to 15° 00′N segment of the East Pacific Rise. *Geochem. Geophys. Geosyst.* **1,** 1011 (2000).
12. Sigmundsson, F., Vadon, H. & Massonnet, D. Readjustment of the Krafla Spreading Segment to crustal rifting measured by satellite radar interferometry. *Geophys. Res. Lett.* **24,** 1843–1846 (1997).
13. Pagli, C., Sigmundsson, F., Árnadóttir, T., Einarsson, P. & Sturkell, E. Deflation of the Askja volcanic system: Constraints on the deformation source from combined inversion of satellite radar interferograms and GPS measurements. *J. Volcanol. Geotherm. Res.* **152,** 97–108 (2006).
14. Wright, T. J. *et al.* Geophysical constraints on the dynamics of spreading centres from rifting episodes on land. *Nature Geosci.* http://dx.doi.org/10.1038/ngeo1420 (in the press, 2012).
15. Barberi, F. & Varet, J. The Erta Ale volcanic range (Danakil Depression, Northern Afar, Ethiopia). *Bull. Volcanol.* **34,** 848–917 (1970).
16. Acocella, V. Regional and local tectonics at Erta Ale caldera, Afar (Ethiopia). *J. Struct. Geol.* **28,** 1808–1820 (2006).
17. McClusky, S. *et al.* Kinematics of the southern Red Sea–Afar Triple Junction and implications for plate dynamics. *Geophys. Res. Lett.* **37,** L05301 (2010).
18. Oppenheimer, C. & Francis, P. Implications of longeval lava lakes for geomorphological and plutonic processes at Erta 'Ale volcano, Afar. *J. Volc. Geother. Res.* **80,** 101–111 (1998).
19. Amelung, F., Oppenheimer, C., Segall, P. & Zebker, H. Ground deformation near Gada 'Ale Volcano, Afar, observed by radar interferometry. *Geophys. Res. Lett.* **27,** 3093–3096 (2000).
20. Belachew, M. *et al.* Comparison of dike intrusions in an incipient seafloor-spreading segment in Afar, Ethiopia: Seismicity perspectives. *J. Geophys. Res.* **116,** B06405 (2011).
21. Wright, R., Flynn, L. P., Garbeil, H., Harris, A. J. L. & Pilger, E. MODVOLC: Near-real-time thermal monitoring of global volcanism. *J. Volc. Geother. Res.* **135,** 29–49 (2004).
22. Yang, K. *et al.* Retrieval of large volcanic SO_2 columns from the Aura Ozone Monitoring Instrument: Comparison and limitations. *J. Geophys. Res.* **112,** D24S43 (2007).
23. Jónsson, S., Zebker, H., Segall, P. & Amelung, F. Fault slip distribution of the 1999 M_w7.2 Hector mine Earthquake, California, estimated from satellite radar and GPS measurements. *Bull. Seismol. Soc. Am.* **92,** 1377–1389 (2002).
24. Grandin, R. *et al.* Transient rift opening in response to multiple dike injections in the Manda Hararo rift (Afar, Ethiopia) imaged by time-dependent elastic inversion of interferometric synthetic aperture radar data. *J. Geophys. Res.* **115,** B09403 (2010).
25. Wright, T. J., Lu, Z. & Wicks, C. Source model for the M_w6.7 23 October 2002 Nenana Mountain Earthquake (Alaska) from InSAR. *Geophys. Res. Lett.* **30,** 1974 (2003).

26. Turcotte, D. L. & Schubert, G. *Geodynamics* 2nd edn, 167–168 (Cambridge Univ. Press, 2002).
27. Ebinger, C. J. & Hayward, N. J. Soft plates and hot spots: Views from Afar. *J. Geophys. Res.* **101,** 21859–21876 (1996).
28. Carbotte, S. M. *et al.* Rift topography linked to magmatism at the intermediate spreading Juan de Fuca. *Geology* **34,** 209–212 (2006).
29. Bastow, I. D. & Keir, D. The protracted development of the continent–ocean transition in Afar. *Nature Geosci.* **4,** 248–250 (2011).
30. Montelli, R. Finite-frequency tomography reveals a variety of plumes in the mantle. *Science* **303,** 338–343 (2004).

Acknowledgements

Our work is supported by Natural Environment Research Council grants NE/D008611/1, NE/D01039X/1 and NE/E007414/1, National Science Foundation grants EAR-0635789 and EAR-0613651 and a Royal Society University Research Fellowship to T.J.W. We are grateful to D. Keir for the help in analysing the seismicity. SAR data copyright ESA from CAT 1 3435. Part of this research was performed at the Jet Propulsion Laboratory, California Institute of Technology under contract with the National Aeronautics and Space Administration. ALOS PALSAR data were provided by Alaska Satellite Facility and the ownership belongs to METI (Ministry of Economy, Trade and Industry) and the Japan Aerospace Exploration Agency.

Author contributions

C.P. processed and modelled the InSAR data, drafted the manuscript and prepared the figures. T.J.W. provided guidance for the modelling and in drafting the paper. He also provided the scripts of the non-uniform contraction/opening models and the Monte-Carlo simulation of correlated noise. C.J.E. did the seismic analysis and interpretation. S-H.Y. processed the ALOS interferogram. J.R.C. provided guidance in drafting the paper, in particular writing the abstract. T.B. analysed the ASTER, OMI and MODIS satellite images and he provided the thermal image of the lava flow in Fig. 1c. A.A. helped to write the paper. All authors contributed to developing the conclusions and implications in the manuscript.

Additional information

The authors declare no competing financial interests. Supplementary information accompanies this paper on www.nature.com/naturegeoscience. Reprints and permissions information is available online at www.nature.com/reprints. Correspondence and requests for materials should be addressed to C.P.